Inorganic Chemistry
Article

*Inorg. Chem.* **2010**, *49*, 519–530 **519**
DOI: 10.1021/ic9017085

# Molecular Dynamics Studies of Concentrated Binary Aqueous Solutions of Lanthanide Salts: Structures and Exchange Dynamics

**Magali Duvail, Alexandre Ruas, Laurent Venault, Philippe Moisy, and Philippe Guilbaud***

*CEA, Nuclear Energy Division, RadioChemistry & Processes Department, F-30207 Bagnols sur Cèze, France*

Received August 28, 2009

Concentrated binary aqueous solutions of lanthanide ($Nd^{3+}$ and $Dy^{3+}$) salts ($ClO_4^-$, $Cl^-$, and $NO_3^-$) have been studied by means of classical molecular dynamics (MD) simulations with explicit polarization and UV−visible spectroscopy. Pair interaction potentials, used for the MD simulations, have been developed in order to reproduce experimental hydration properties. $Nd^{3+}$ and $Dy^{3+}$ have been chosen because of their position in the lanthanide series: $Nd^{3+}$ being a light lanthanide and $Dy^{3+}$ a heavy one. They are respectively coordinated to nine and eight water molecules, in pure water, involving changes in their salt hydration structures. Both MD simulations and UV−visible experiments highlight the stronger affinity of nitrate anions toward $Ln^{3+}$ compared to perchlorates and chlorides. Dissociation/association processes of $Nd^{3+}-Cl^-$ and $Nd^{3+}-NO_3^-$ ion pairs in aqueous solution have been analyzed using potential of mean force profile calculations. Furthermore, from MD simulations, it appears that the affinity of anions (perchlorate, chloride, and nitrate) is stronger for $Nd^{3+}$ than $Dy^{3+}$.

## 1. Introduction

Structural characterization remains full of twists and turns when it relates to water solutions. Actually, even for simple metallic cation salts, no single experiment allows provision of a full description of their first and second coordination shell structural properties (distances, coordination numbers, and coordination modes, etc.). Understanding the hydration structure of these metal ions in aqueous solution is, however, the first step to address their solvation properties and chemical reactivity.

Although a lot of experimental[1−6] and theoretical[7−11] studies on heavy atoms in aqueous solutions, such as lanthanides ($Ln^{3+}$) and actinides ($An^{3+}$), have been performed over the past decades, their characterization remains to be achieved, especially in the presence of counteranions. For instance, some questions have remained until now, without an unambiguous answer, about the geometries of common lanthanide salts with chloride, perchlorate, or nitrate in these solutions. Are these salts inner-sphere-associated in water? How does the increase of salt concentrations affect (i) this association and (ii) the two first cation coordination shell structures? Such matters may be addressed combining both theoretical calculations and experiments,[12,13] as we previously did for $DyCl_3$ salt using molecular dynamic simulations, extended X-ray absorption fine structure (EXAFS), UV−visible/near-IR, and time-resolved laser-induced fluorescence spectroscopies.[14] Although no influence of the concentration has been observed for this salt, the structural and thermodynamic properties of solutions with different counterions may change because of the very high concentrations of $Ln^{3+}$ salts.[15−17]

Molecular dynamics (MD), using the classical, ab initio, or mixed quantum/classical interaction potential, is a method of

*To whom correspondence should be addressed. E-mail: philippe.guilbaud@cea.fr.

(1) Cossy, C.; Helm, L.; Merbach, A. E. *Inorg. Chem.* **1988**, *27*, 1973–1979.
(2) Fanghänel, T.; Kim, J. I.; Klenze, R.; Kato, Y. *J. Alloys Compd.* **1995**, *225*, 308–311.
(3) Näslund, J.; Lindqvist-Reis, P.; Persson, I.; Sandström, M. *Inorg. Chem.* **2000**, *39*, 4006–4011.
(4) Allen, P.; Bucher, J. J.; Shuh, D. K.; Edelstein, N. M.; Craig, I. *Inorg. Chem.* **2000**, *39*, 595–601.
(5) D'Angelo, P.; De Panfilis, S.; Filipponi, A.; Persson, I. *Chem.—Eur. J.* **2008**, *14*, 3045–3055.
(6) Skerencak, A.; Panak, P. J.; Hauser, W.; Neck, V.; Klenze, R.; Lindqvist-Reis, P.; Fanghänel, T. *Radiochim. Acta* **2009**, *97*, 385–393.
(7) Kowall, T.; Foglia, F.; Helm, L.; Merbach, A. E. *J. Am. Chem. Soc.* **1995**, *117*, 3790–3799.
(8) Floris, F. M.; Tani, A. *J. Chem. Phys.* **2001**, *115*, 4750–4765.
(9) Clavaguéra, C.; Pollet, R.; Soudan, J. M.; Brenner, V.; Dognon, J. P. *J. Phys. Chem. B* **2005**, *109*, 7614–7616.
(10) Duvail, M.; Vitorge, P.; Spezia, R. *J. Chem. Phys.* **2009**, *130*, 104501–13.
(11) Villa, A.; Hess, B.; Saint-Martin, H. *J. Phys. Chem. B* **2009**, *113*, 7270–7281.
(12) Spezia, R.; Duvail, M.; Vitorge, P.; Cartailler, T.; Tortajada, J.; D'Angelo, P.; Gaigeot, M.-P. *J. Phys. Chem. A* **2006**, *110*, 13081–13088.
(13) Duvail, M.; D'Angelo, P.; Gaigeot, M.-P.; Vitorge, P.; Spezia, R. *Radiochim. Acta* **2009**, *97*, 339–346.
(14) Ruas, A.; Guilbaud, P.; Den Auwer, C.; Moulin, C.; Simonin, J.-P.; Turq, P.; Moisy, P. *J. Phys. Chem. A* **2006**, *110*, 11770–11779.
(15) Silva, R.; Bidoglio, G.; Rand, M.; Robouch, P.; Wanner, H.; Puigdomenech, I. *Chemical Thermodynamics of Americium*; OECD, **2004**.
(16) Vitorge, P.; Capdevila, H. *Radiochim. Acta* **2003**, *91*, 623–631.
(17) Vitorge, P.; Phrommavanh, V.; Siboulet, B.; You, D.; Vercouter, T.; Descostes, M.; Marsden, C. J.; Beaucaire, C.; Gaudet, J.-P. *C. R. Chim.* **2007**, *10*, 978–993.


Published on Web 12/21/2009

choice to determine structural and dynamical properties in solution since it is able to simulate real experimental conditions.[12,18−22] It has been clearly established now that the average distance between $Ln^{3+}$ and the water molecules of the first shell decreases continuously through the series, involving a change in the coordination number (CN), going from nine for the lightest $Ln^{3+}$ to eight for the heaviest ones.[7,23−25] Moreover, Helm and Merbach proposed water self-exchange mechanisms depending on the reaction pathway: (i) a concerted-associative one for the 9 → 8 reaction (predominant for heavy $Ln^{3+}$) and (ii) a concerted-dissociative one for the 8 → 9 reaction pathway.[23] Thus, different water self-exchange mechanisms may lead to changes in the $Ln^{3+}$ salt hydration properties depending on the position of the studied $Ln^{3+}$ in the series.

Classical[7,8,10,14,23,26,27] and Car−Parrinello (CPMD)[21,28] MD simulations have frequently been used as theoretical approaches in providing a representation of $Ln^{3+}$ solvation properties in diluted aqueous solutions. A recent CPMD study on $La^{3+}$ in a highly concentrated LiCl solution (14 mol $L^{-1}$)[29] highlights the presence of two $Cl^-$ anions in the $La^{3+}$ first coordination shell in good agreement with published EXAFS data.[4] However, at this LiCl concentration, the inner-sphere association between $Cl^-$ anions and $La^{3+}$ may be explained with the very high number of $Cl^-$'s in the solution (seven per $Ln^{3+}$). Some MD simulation studies are also reported in the literature for $Ln(NO_3)_3$ salts. Hirata and Dobler studied the complexation between $Ln^{3+}$ and organic ligands in water and in organic solvent in the presence of nitrate counteranions.[30] Wipff and coworkers also did a lot of simulations including these salts in different media (water, water/chloroform interface, ionic liquids, supercritical $CO_2$).[31−35] However, all of these MD simulations were performed with a force field that does not include explicit polarization, while it is now well-known that explicit polarization is crucial to have a good representation of $Ln^{3+}$ hydration properties.[7,27,36]

From an experimental point of view, $Ln^{3+}$ complexations with anions, like chloride[4,37−41] or nitrate,[38,42−45] are often studied in order to determine stability constants. It is now established that lanthanide cations do not form inner-sphere complexes with perchlorate anions, which makes them suitable for EXAFS spectroscopy to determine ion hydration properties.[3,46] Indeed, Näslund et al.[3] determined by EXAFS spectroscopy the $La^{3+}-O_{water}$ distance from a $La(ClO_4)_3$ aqueous solution with a $[ClO_4^-]/[La^{3+}]$ ratio of 6 (concentration estimated at 1 mol $kg^{-1}$ from the solution density using ref 47). Lindqvist-Reis et al. also determined EXAFS $M^{3+}-O_{water}$ distances from solutions with a $[ClO_4^-]/[M^{3+}]$ ratio of 3−3.5.[46] Thus, it should be kept in mind that ion structural properties are determined from solutions looking like the simulation box in Figure 1b), that is, with a rather high density of ions in water. For chloride anions, experimental data with $Ln^{3+}$ cations show that (i) the Ln−Cl interaction is weak and may involve an inner-sphere complexation only at high concentration[14,41] and (ii) this interaction decreases in the lanthanide series.[4] The case of nitrate ions is quite different. It is well-known that these anions coordinate lanthanide ions in their first coordination shell,[39] but their coordination mode (bi- versus monodentate) toward $Ln^{3+}$ cations in aqueous solution is still debated[42,45,48] since no experimental data allow today to give an irrevocable choice between these two modes.

However, although all of these experimental techniques provide reliable structural (distance in the first coordination shell) and thermodynamic (stability and association constants) data, there is still a lack of description of the microscopic environment of these ions in solution, especially of their second coordination shell.

Among the theories for describing thermodynamical properties (like the Pitzer theory, SIT model), the binding mean spherical approximation (BIMSA) is promising for its predictive capabilities for the description of binary solutions.[49−51] An optimum use of the BIMSA theory requires a good understanding of the microscopic features of binary solutions, that is, an accurate description of the two first cation coordination shells. Experimental methods adapted for this description being scarce

(18) Hofer, T. S.; Tran, H. T.; Schwenk, C. F.; Rode, B. M. *J. Comput. Chem.* **2004**, *25*, 211–217.
(19) Rode, B. M.; Hofer, T. S. *Pure Appl. Chem.* **2006**, *78*, 525–539.
(20) Duvail, M.; Spezia, R.; Cartailler, T.; Vitorge, P. *Chem. Phys. Lett.* **2007**, *448*, 41–45.
(21) Yazyev, O. V.; Helm, L. *J. Chem. Phys.* **2007**, *127*, 084506–8.
(22) Spezia, R.; Bresson, C.; Den Auwer, C.; Gaigeot, M.-P. *J. Phys. Chem. B* **2008**, *112*, 6490–6499.
(23) Helm, L.; Merbach, A. E. *Chem. Rev.* **2005**, *105*, 1923–1960.
(24) Persson, I.; D'Angelo, P.; De Panfilis, S.; Sandström, M.; Eriksson, L. *Chem.—Eur. J.* **2008**, *14*, 3056–3066.
(25) Duvail, M.; Spezia, R.; Vitorge, P. *Chem. Phys. Chem.* **2008**, *9*, 693–696.
(26) Clavaguera, C.; Calvo, F.; Dognon, J.-P. *J. Chem. Phys.* **2006**, *124*, 074505.
(27) Duvail, M.; Souaille, M.; Spezia, R.; Cartailler, T.; Vitorge, P. *J. Chem. Phys.* **2007**, *127*, 034503–11.
(28) Ikeda, T.; Hirata, M.; Kimura, T. *J. Chem. Phys.* **2005**, *122*, 244507.
(29) Petit, L.; Vuilleumier, R.; Maldivi, P.; Adamo, C. *J. Phys. Chem. B* **2008**, *112*, 10603–10607.
(30) Dobler, M.; Hirata, M. *Phys. Chem. Chem. Phys.* **2004**, *6*, 1672–1678.
(31) Beudaert, P.; Lamare, V.; Dozol, J.; Troxler, L.; Wipff, G. *J. Chem. Soc., Perkin Trans. 2* **1999**, 2515–2523.
(32) Schurhammer, R.; Berny, F.; Wipff, G. *Phys. Chem. Chem. Phys.* **2001**, *3*, 647–656.
(33) Baaden, M.; Berny, F.; Madic, C.; Schurhammer, R.; Wipff, G. *Solvent Extr. Ion Exch.* **2003**, *21*, 199–220.
(34) Chaumont, A.; Wipff, G. *Phys. Chem. Chem. Phys.* **2003**, *5*, 3481–3488.
(35) Diss, R.; Wipff, G. *Phys. Chem. Chem. Phys.* **2005**, *7*, 264–272.
(36) Salanne, M.; Simon, C.; Turq, P.; Madden, P. A. *J. Phys. Chem. B* **2008**, *112*, 1177–1183.
(37) Reidler, J.; Silber, H. B. *J. Phys. Chem.* **1974**, *78*, 424–428.
(38) Reuben, J. *J. Phys. Chem.* **1975**, *79*, 2154–2157.
(39) Annis, B. K.; Hahn, R. L.; Narten, A. H. *J. Chem. Phys.* **1985**, *82*, 2086–2091.
(40) Yaita, T.; Narita, H.; Suzuki, S.; Tachimori, S.; Motohashi, H.; Shiwaku, H. *J. Radioanal. Nucl. Chem.* **1999**, *239*, 371–375.
(41) Soderholm, L.; Skanthakumar, S.; Wilson, R. E. *J. Phys. Chem. A* **2009**, *113*, 6391–6397.
(42) Bonal, C.; Morel, J.-P.; Morel-Desrosiers, N. *J. Chem. Soc. Faraday Trans.* **1996**, *92*, 4957–4963.
(43) Bonal, C.; Morel, J.-P.; Morel-Desrosiers, N. *J. Chem. Soc. Faraday Trans.* **1998**, *94*, 1431–1436.
(44) Andersson, S.; Eberhardt, K.; Ekberg, C.; Liljenzin, J.-O.; Nilsson, M.; Skarnemark, G. *Radiochim. Acta* **2006**, *94*, 469–474.
(45) Rao, L.; Tian, G. *Inorg. Chem.* **2009**, *48*, 964–970.
(46) Lindqvist-Reis, P.; Munoz-Paez, A.; Diaz-Moreno, S.; Pattanaik, S.; Persson, I.; Sandstrom, M. *Inorg. Chem.* **1998**, *37*, 6675–6683.
(47) Spedding, F. H.; Shiers, L. E.; Brown, M. A.; Derer, J. L.; Swanson, D. L.; Habenschuss, A. *J. Chem. Eng. Data* **1975**, *20*, 81–88.
(48) Dobler, M.; Guilbaud, P.; Dedieu, A.; Wipff, G. *New J. Chem.* **2001**, *25*, 1458–1465.
(49) Simonin, J.-P.; Bernard, O.; Blum, L. *J. Phys. Chem. B* **1999**, *103*, 699–704.
(50) Ruas, A.; Moisy, P.; Simonin, J.-P.; Bernard, O.; Dufreche, J.; Turq, P. *J. Phys. Chem. B* **2005**, *109*, 5243–5248.
(51) Ruas, A.; Bernard, O.; Caniffi, B.; Simonin, J.-P.; Turq, P.; Blum, L.; Moisy, P. *J. Phys. Chem. B* **2006**, *110*, 3435–3443.

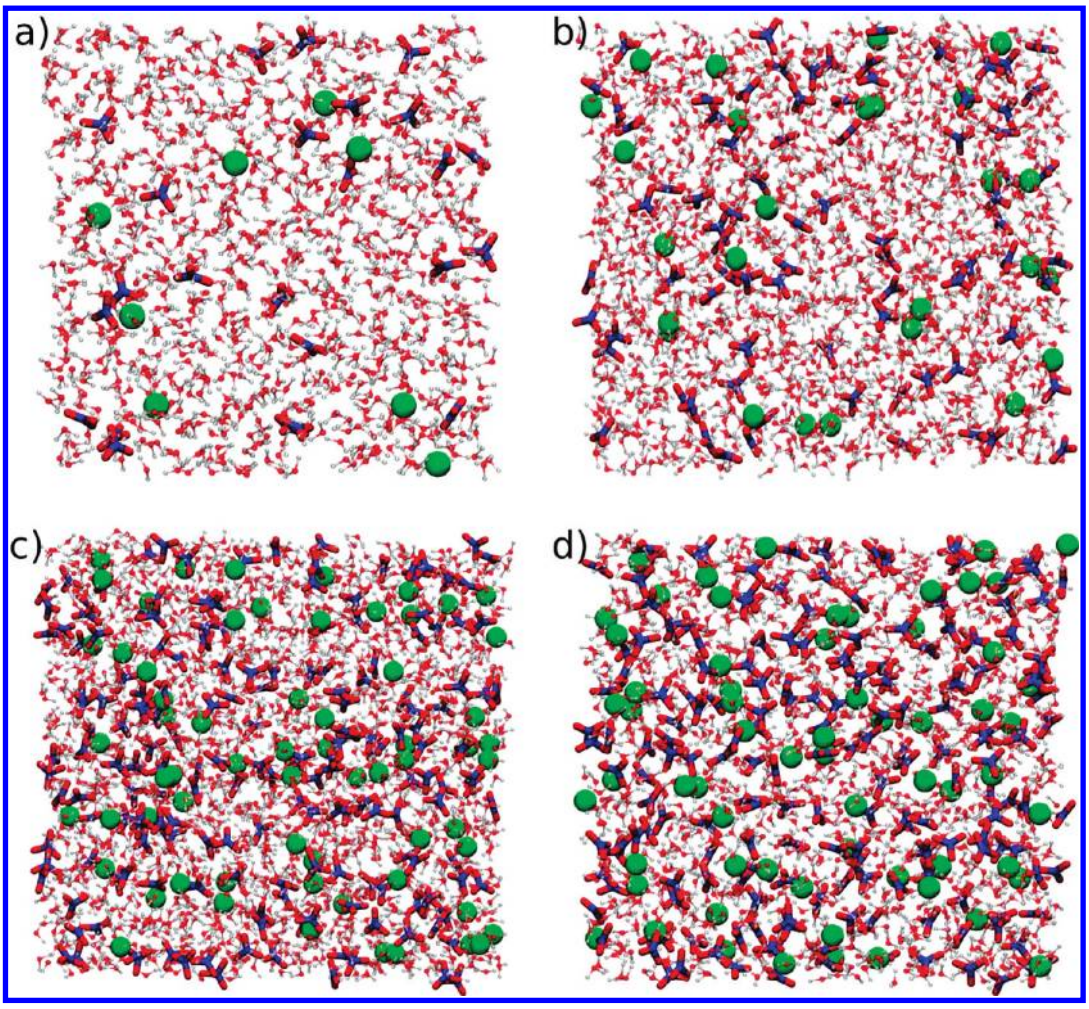


**Figure 1.** $Nd^{3+}$ (green) nitrate salt simulation boxes at the different studied concentrations: (a) 0.5 mol $kg^{-1}$, (b) 1.0 mol $kg^{-1}$, (c) 2.0 mol $kg^{-1}$, and (d) 3.0 mol $kg^{-1}$.

and difficult to conduct, MD simulations are a promising alternative: they offer a global microscopic description of a given system, beyond the first coordination shell of a given ion.

In the present work, we report, for the first time, a molecular dynamics study, including explicit polarization, on binary aqueous solutions of two $Ln^{3+}$ ($Nd^{3+}$ and $Dy^{3+}$) salts ($Cl^-$, $NO_3^-$, and $ClO_4^-$) for concentrations varying from a "highly diluted" solution to 3 mol $kg^{-1}$ of a solvent (i.e., close to the experimental saturation). Chloride, nitrate, and perchlorate anions have been chosen as counteranions since they are the most common counteranions used experimentally: chlorides and nitrates are actually involved in lanthanide separation processes, and perchlorates are generally used as reference (nonbonding) counterions for many experiments.[3,46] As mentioned above, changes in the $Ln^{3+}$ hydration properties (decrease of the coordination number, changes in water self-exchange mechanisms) through the series may lead to differences in the $Ln^{3+}$ salt hydration properties. Thus, $Nd^{3+}$ and $Dy^{3+}$ have been chosen because of their position in the $Ln^{3+}$ series: $Nd^{3+}$ being a light lanthanide coordinated to nine water molecules and $Dy^{3+}$ a heavy one coordinated to eight water molecules (in diluted aqueous solutions). Furthermore, since $Nd^{3+}$ and $Dy^{3+}$ absorb in the UV−visible/near-IR region, MD simulations were compared to UV−visible experiments to check the validity of our model, as previously done on $DyCl_3$.[14]

## 2. Methods

**2.1. Molecular Dynamics Simulations.** MD simulations of lanthanide ($Ln^{3+} = Nd^{3+}$ and $Dy^{3+}$) salt concentrated aqueous solutions have been carried out with SANDER8, a module of AMBER8,[52] using explicit polarization in the *NPT* ensemble. Periodic boundary conditions were applied to the simulation box. Long-range interactions have been calculated using the particle-mesh Ewald method.[53] Equations of motion were numerically integrated using a 1 fs time step. Systems were previously equilibrated at room temperature over at least 100 ps, and production runs were subsequently collected for 2 ns.

The van der Waals energy is described here by a 12−6 Lennard-Jones (LJ) potential. The $\varepsilon_{ij}$ and $\sigma_{ij}$ LJ potential parameters were determined to reproduce experimental structural properties of ions in aqueous solutions, that is, $Nd^{3+}$, $Dy^{3+}$, $Cl^-$, $NO_3^-$, and $ClO_4^-$ properties (Table 1).

Water molecules were described by the rigid POL3 model,[54,55] which takes into account the polarization. LJ parameters for the

(52) Case, D. A. et al. *AMBER 8*; University of California: San Francisco, CA.
(53) Darden, T.; York, D.; Pedersen, L. *J. Chem. Phys.* **1993**, *98*, 10089–10092.
(54) Caldwell, J. W.; Kollman, P. A. *J. Phys. Chem.* **1995**, *99*, 6208–6219.
(55) Meng, E.; Kollman, P. *J. Phys. Chem.* **1996**, *100*, 11460–11470.

**Table 1.** Parameters Used for the MD Simulations[a]

| ion/water | $\varepsilon_{ii}$ | $\sigma_{ii}$ | $q_i$ | α |
|---|---|---|---|---|
| $Nd^{3+}$ | 0.297 | 3.430 | +3.000 | 0.955[b] |
| $Dy^{3+}$ | 0.331 | 3.118 | +3.000 | 0.728[b] |
| $O_W$[c] | 0.625 | 3.204 | −0.730 | 0.528 |
| $H_W$[c] | | | +0.365 | 0.170 |
| $Cl^-$ | 0.418 | 4.401 | −1.000 | 3.235 |
| $N_N$[d] | 0.711 | 3.250 | +0.896 | 0.530 |
| $O_N$[d] | 0.879 | 2.960 | −0.632 | 0.434 |
| $Cl_P$[e] | 1.109 | 3.471 | +0.580 | 1.910 |
| $O_P$[e] | 0.879 | 2.958 | −0.395 | 0.434 |

[a] Energies are in kJ $mol^{-1}$, distances in Å, and atomic polarizabilities in $Å^3$. [b] Atomic polarizabilities were taken from ref 63. [c] Subscript W for water. [d] Subscript N for nitrate. [e] Subscript P for perchlorate.

$Ln^{3+}$ ions (Table 1) were determined to reproduce experimental hydration properties, that is, (i) for $Nd^{3+}$, nine water molecules with a Nd−$O_W$ distance in the range of 2.48−2.52 Å,[4,5,24,56−61] and (ii) for $Dy^{3+}$, eight water molecules with a Dy−$O_W$ distance in the range 2.37−2.40 Å.[5,39,59,61,62] Atomic polarizabilities used for the $Ln^{3+}$ ions have been calculated by Clavaguéra and Dognon.[63] These sets of parameters for $Nd^{3+}$ and $Dy^{3+}$ provide results in good agreement with experimental data: 8.8 water molecules at 2.52 Å and eight water molecules at 2.39 Å for $Nd^{3+}$ and $Dy^{3+}$, respectively. Although no reliable experimental values are available for the $Ln^{3+}$ second hydration shell properties, Ln−O distances and coordination numbers are consistent with other computed values,[25] that is, 20 water molecules at 4.73 Å and 18 water molecules at 4.59 Å, for $Nd^{3+}$ and $Dy^{3+}$, respectively. Mean residence times (MRTs) of water molecules in the $Ln^{3+}$ first hydration shells, calculated using the same formalism as in ref 27, are also in good agreement with those calculated in refs 10 and 25, that is, on the order of a nanosecond.

The $Cl^-$ anion was described by the polarizable model defined by Smith and Dang.[64] These parameters provide structural properties in good agreement with experimental structural data:[65,66] seven water molecules with a Cl−$O_W$ distance of 3.2 Å. The model defined by Velardez et al.[67] to describe the $NO_3^-$ anion was used with partial atomic charges ($q_{O_N}$ and $q_{N_N}$) calculated with the restricted electrostatic potential procedure of Bayly et al.[68] These parameters provide structural properties for $NO_3^-$ in liquid water in reasonable agreement with experimental[69] and calculated[70] structural data ($N_N$−$O_W$ = 3.4 Å), that is, six to seven water molecules in the nitrate first hydration shell at a N−$O_W$ distance of 3.6 Å. To our knowledge, no polarizable model for the $ClO_4^-$ anion is available in the literature; thus atomic partial charges ($q_{Cl_P}$ and $q_{O_P}$) of the nonpolarizable models of the perchlorate anion used by Liu et al.[71] were modified, as is generally done.[27,54,72,73] From these parameters, we calculated six to seven water molecules in the perchlorate anion's first hydration shell with a Cl−$O_W$ distance of 3.60 Å, consistent with an experimental value determined by large-angle X-ray scattering (3.66 Å).[46]

**Table 2.** Characteristics of the Simulation Boxes for Concentrated Aqueous Solutions of Lanthanide Salts

| | $N(Ln^{3+})$[a] | $N(A^-)$[b] | $N(H_2O)$[c] | $R(H_2O/Ln^{3+})$[d] |
|---|---|---|---|---|
| Sim(D) | 1 | 3 | 2138 | 2138 |
| Sim(0.5) | 8 | 24 | 887 | 111 |
| Sim(1) | 27 | 81 | 1498 | 55.5 |
| Sim(2) | 64 | 192 | 1776 | 27.75 |
| Sim(3) | 64 | 192 | 1184 | 18.5 |

[a] Number of $Ln^{3+}$ ions in the simulation box. [b] Number of anions ($Cl^-$ or $NO_3^-$ or $ClO_4^-$) in the simulation box. [c] Number of water molecules in the simulation box. [d] Number of water molecules per $Ln^{3+}$ ion.

Simulations of $Ln^{3+}$ ($Nd^{3+}$ and $Dy^{3+}$) salt ($Cl^-$, $ClO_4^-$, and $NO_3^-$) binary solutions were performed at different concentrations (from high dilution to 3 mol per kilogram of water, noted mol $kg^{-1}$) at room temperature. Simulations of the highly diluted solution (Sim(D)) were performed from different starting geometries, because the association or dissociation process of the anion in the vicinity of $Ln^{3+}$ may occur at time scales longer than those easily reachable (some nanoseconds) in MD simulations. These simulation boxes were built from an equilibrated water box in which one $Ln^{3+}$ and three anions were included. The anions may either be (i) in the $Ln^{3+}$ first coordination shell or (ii) in the bulk (in the second coordination shell or at higher distances).

For the 0.5 (Sim(0.5)), 1.0 (Sim(1)), 2.0 (Sim(2)), and 3.0 mol $kg^{-1}$ (Sim(3)) concentrations, all of the lanthanide salts were built as first shell dissociated salts, that is, $Ln^{3+}$, $3A^-$, because the total dissociation of the three anions occurs on a time scale longer than our simulation time (Table 2). Densities of the simulated binary solutions are in good agreement with the experimental ones[47,74,75] (Supporting Information Tables S1 and S2).

**2.2. Potentials of Mean Force.** Potentials of mean force (PMFs) of $Nd^{3+}$−$Cl^-$ and $Nd^{3+}$−$NO_3^-$ in water were calculated from umbrella-sampling simulations.[76] The umbrella-sampling method introduces a biasing potential in the force field to sample some regions or windows around an "equilibrium" reaction coordinate. The reaction coordinate here is the solute−solute distance, that is, the $Nd^{3+}$−$Cl^-$ or $Nd^{3+}$−$N_{NO_3^-}$ distance. The umbrella-sampling molecular dynamics simulations were carried out with a harmonic restraining potential using a force constant equal to 3.4 $k_BT$ $Å^{-2}$. The solute−solute "equilibrium" distance for a given window varies from 2.0 to 12.0 Å for $Cl^-$, and from 2.0 to 11.0 Å for $NO_3^-$, with a 0.5 Å step. For the $Nd^{3+}$−$Cl^-$ PMF calculations, some umbrella-sampling MD simulations had to be performed with a higher

(56) Habenschuss, A.; Spedding, F. H. *J. Chem. Phys.* **1979**, *70*, 3758–3763.
(57) Narten, A. H.; Hahn, R. L. *Science* **1982**, *217*, 1249–1250.
(58) Narten, A. H.; Hahn, R. L. *J. Phys. Chem. B* **1983**, *87*, 3193–3197.
(59) Helm, L.; Foglia, F.; Kowall, T.; Merbach, A. E. *J. Phys.: Condens. Matter* **1994**, *6*, A137–A140.
(60) Solera, J. A.; Garcia, J.; Proietti, M. G. *Phys. Rev. B* **1995**, *51*, 2678–2686.
(61) Ishiguro, S.-I.; Umebayashi, Y.; Kato, K.; Takahashib, R.; Ozutsumi, K. *J. Chem. Soc., Faraday Trans.* **1998**, *94*, 3607–3612.
(62) Habenschuss, A.; Spedding, F. H. *J. Chem. Phys.* **1979**, *70*, 2797–2806.
(63) Clavaguéra, C.; Dognon, J. *Chem. Phys.* **2005**, *311*, 169–176.
(64) Smith, D. E.; Dang, L. X. *J. Chem. Phys.* **1994**, *100*, 3757–3766.
(65) Caminiti, R.; Licheri, G.; Paschina, G.; Piccaluga, G.; Pinna, G. *J. Chem. Phys.* **1980**, *72*, 4522–4528.
(66) Mason, P. E.; Ansell, S.; Neilson, G. W.; Brady, J. W. *J. Phys. Chem. B* **2008**, *112*, 1935–1939.
(67) Velardez, G. F.; Alavi, S.; Thompson, D. L. *J. Chem. Phys.* **2004**, *120*, 9151–9159.
(68) Bayly, C. I.; Cieplak, P.; Cornell, W.; Kollman, P. A. *J. Phys. Chem.* **1993**, *97*, 10269–10280.
(69) Caminiti, R.; Licheri, G.; Piccaluga, G.; Pinna, G. *J. Chem. Phys.* **1978**, *68*, 1967–1970.
(70) Dang, L. X.; Chang, T.-M.; Roeselova, M.; Garrett, B. C.; Tobias, D. J. *J. Chem. Phys.* **2006**, *124*, 066101–3.
(71) Liu, X.; Zhang, S.; Zhou, G.; Wu, G.; Yuan, X.; Yao, X. *J. Phys. Chem. B* **2006**, *110*, 12062–12071.
(72) Caldwell, J.; Dang, L. X.; Kollman, P. A. *J. Am. Chem. Soc.* **1990**, *112*, 9144–9147.
(73) Armunanto, R.; Schwenk, C. F.; Setiaji, A. H. B.; Rode, B. M. *Chem. Phys.* **2003**, *295*, 63–70.
(74) Spedding, F. H.; Saeger, V. W.; Gray, K. A.; Boneau, P. K.; Brown, M. A.; DeKock, C. W.; Baker, J. L.; Shiers, L. E.; Weber, H. O.; Habenschuss, A. *J. Chem. Eng. Data* **1975**, *20*, 72–81.
(75) Spedding, F. H.; Shiers, L. E.; Brown, M. A.; Baker, J. L.; Guitierrez, L.; McDowell, L. S.; Habenschuss, A. *J. Phys. Chem.* **1975**, *79*, 1087–1096.
(76) Torrie, G. M.; Valleau, J. P. *J. Comp. Phys.* **1977**, *23*, 187–199.

force constant (16.8 $k_BT$ Å$^{-2}$) at the Nd−Cl = 3.25, 3.5, and 3.75 Å distances. These umbrella-sampling simulation protocols have been optimized to ensure a good overlap of the equilibrium windows, and therefore a good representation of the reaction pathways. All of these simulations have been performed with SANDER8[52] in the *NVT* ensemble at 300 K. Systems were previously equilibrated at room temperature for at least 10 ps for each windows. Production runs were subsequently collected for 500 ps to 1 ns. Then, free-energy calculations were performed using the weighted histogram analysis method.[77,78]

**2.3. UV−Visible Experiments.** Spectroscopic measurements were performed to study the first coordination sphere of $Nd^{3+}$ and $Dy^{3+}$, in particular for highly concentrated binary solutions. It is well-known that, according to the Judd−Ofelt theory, modification of the first coordination shell of a given ion can change the features of UV−visible/near-IR spectra (absorption wavelength, fwhm, and molar extinction coefficient).

$NdCl_3$, $Nd(NO_3)_3$, and $Dy(NO_3)_3$ concentrated solutions were prepared by dissolving, in deionized water, weighted quantities of the corresponding salts (Aldrich, 99.9% pure). A very low amount of acid (HCl or $HNO_3$) was added to obtain total dissolution. However, the added proportion of acid was weak enough to consider the $NdCl_3$, $Nd(NO_3)_3$, and $Dy(NO_3)_3$ solutions as binary solutions. The concentrations of these binary salt solutions were verified from UV−visible spectra of each sample, diluted in $HClO_4$ to 1 mol $L^{-1}$. Conversion from the moles per liter scale to moles per kilogram scale was done using density data from refs 74 and 75. The $NdCl_3$, $Nd(NO_3)_3$, and $Dy(NO_3)_3$ concentrations were respectively 3.1, 2.7, and 2.7 mol $kg^{-1}$. $Nd(NO_3)_3$ has been diluted to obtain solutions of concentrations 2.0, 1.0, and 0.6 mol $kg^{-1}$.

For comparison, ternary neodymium perchlorate−perchloric acid solutions (Aldrich, $[Nd(ClO_4)_3]$ = 1.3 mol $L^{-1}$) and dysprosium perchlorate−perchloric acid solutions (Aldrich, $[Dy(ClO_4)_3]$ = 1.5 mol $L^{-1}$) were used.

UV−visible−near-infrared absorption spectrophotometry measurements were performed using a dual-beam, double monochromator spectrophotometer (Shimadzu UVPC 3101) and using Hellma Suprasil quartz vessels (optical path length from 0.05 to 1 cm). The spectra were recorded at room temperature, between 300 and 1300 nm.

## 3. Results

**3.1. Exchange Dynamics of Anions in Highly Diluted Solutions.** Simulations of first-shell-associated lanthanide salts were first performed at a high dilution in order to estimate the salt dissociation time scale, and thus the exchange dynamics between water molecules and anions in the $Ln^{3+}$ first coordination shell.

**3.1.1. Lanthanide Perchlorates.** Simulations starting from first-shell-associated perchlorate salts, for both $Nd^{3+}$ and $Dy^{3+}$, highlight three possible coordination modes in their first hydration shell, (i) tridentate with calculated Ln−Cl distances of 2.81 and 2.56 Å for $Nd^{3+}$ and $Dy^{3+}$, respectively, (ii) bidentate with calculated Ln−Cl distances of 3.05 and 2.96 Å for $Nd^{3+}$ and $Dy^{3+}$, respectively, and (iii) monodentate with calculated Ln−Cl distances of 3.82 and 3.78 Å for $Nd^{3+}$ and $Dy^{3+}$, respectively. Although the same coordination modes are observed for light and heavy lanthanides, ratios of these modes are different. At the end of the simulation (after 2 ns), the three perchlorate anions are still present in the first hydration shell of $Nd^{3+}$, whereas one perchlorate anion has left the $Dy^{3+}$ first hydration shell after about 200 ps. It appears that the tridentate conformation might be more stable in the case of $Nd^{3+}$ compared to $Dy^{3+}$. Moreover, the departure of the perchlorate anion from the first hydration shell of $Dy^{3+}$ shows that the $ClO_4^-$ anion adopts the three mentioned conformations before it leaves, that is, tridentate, then bidentate, and finally monodentate. The $ClO_4^-$ anion can be replaced by a water molecule only in the latter conformation, the exchange time being rather fast (1−2 ps). Although few monodentate conformations are observed for $Nd^{3+}$ (about 4%), the probability of a (complete) dissociation of the salt is low within the simulation time range. Nevertheless, since this can be observed for $Dy^{3+}$, we may suppose that, for longer simulations, perchlorate anions will be replaced one-by-one by water molecules, for both $Nd^{3+}$ and $Dy^{3+}$. Moreover, when starting the simulation from a first-shell-dissociated point, perchlorates are observed in the cation's second coordination shell, but they never enter its first shell. The absence of first shell association between $Ln^{3+}$ and perchlorates is here not due to the slow diffusion of anions in the solution. Indeed, it takes up to 500 ps for a perchlorate anion to travel from the bulk (25−30 Å) to the $Ln^{3+}$ second coordination shell. The dissociated salt might be then more stable than the first-shell-associated one in water.

**3.1.2. Lanthanide Chlorides.** Simulations of one $LnCl_3$ in water, as for lanthanide perchlorate, were performed in order to estimate the salt dissociation time scale. No dissociation was observed during the 2 ns simulation, neither for $Nd^{3+}$ nor for $Dy^{3+}$ . In these simulations, the three $Cl^-$'s are located in the $Ln^{3+}$ first coordination shell at 2.68 and 2.58 Å for $Nd^{3+}$ and $Dy^{3+}$, respectively, in good agreement with experimental values obtained for the $Nd(bipy)_2Cl_3-CH_3OH$ solid (2.74−2.80 Å)[79] and molten salts of $NdCl_3$ (nine $Cl^-$'s at 2.87 Å and six $Cl^-$'s at 2.77 Å).[80] The presence of $Cl^-$ anions in the $Ln^{3+}$ first coordination shell results in a low number of water molecules in this shell, that is, three water molecules at 2.52 and 2.42 Å, for $Nd^{3+}$ and $Dy^{3+}$, respectively. Note that the total coordination number for both $Ln^{3+}$'s in these cases is six, but the $Dy-O_w$ distance calculated here in the first coordination shell is larger than the one calculated for the octaaqua ion in pure liquid water (2.39 Å). However, for both $Ln^{3+}$'s, the total coordination number is smaller than those calculated in pure liquid water (nine for $Nd^{3+}$ and eight for $Dy^{3+}$). As observed for perchlorates when starting from a first-shell-dissociated salt, $Cl^-$ anions are also found in the $Ln^{3+}$ second coordination shell, without entering its first shell. As for perchlorates, chloride diffusion in solution is not responsible for the nonassociation between $Cl^-$ and $Ln^{3+}$, since it takes 100 and 200 ps to travel about 16 Å for $Nd^{3+}$ and $Dy^{3+}$, respectively.

**3.1.3. Lanthanide Nitrates.** First-shell-associated lanthanide nitrates were simulated to estimate the salt dissociation time scale. The three nitrate anions coordinated

(77) Kumar, S.; Rosenberg, J. M.; Bouzida, D.; Swendsen, R. H.; Kollman, P. A. *J. Comput. Chem.* **1992**, *13*, 1011–1021.

(78) Kumar, S.; Rosenberg, J. M.; Bouzida, D.; Swendsen, R. H.; Kollman, P. A. *J. Comput. Chem.* **1995**, *16*, 1339–1350.

(79) Singh, U. P.; Kumar, R. *J. Mol. Struct.* **2007**, *837*, 214–223.

(80) Matsuura, H.; Watanabe, S.; Sakamoto, T.; Kanuma, T.; Naoi, K.; Hatcho, M.; Kitamura, N.; Akatsuka, H.; Adya, A.; Honma, T.; Uruga, T.; Umesaki, N. *J. Alloys Compd.* **2006**, *408−412*, 80−83; Proceedings of Rare Earths '04 in Nara, Japan, Proceedings of Rare Earths '04.

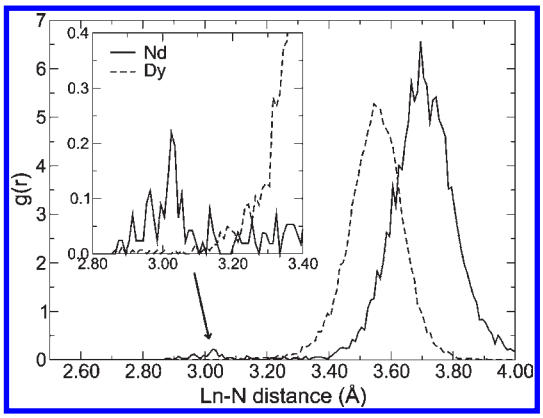


**Figure 2.** Ln−N radial distribution functions obtained from first shell associated lanthanide nitrate salts in highly diluted solution for $Nd^{3+}$ (solid line) and $Dy^{3+}$ (dashed line).

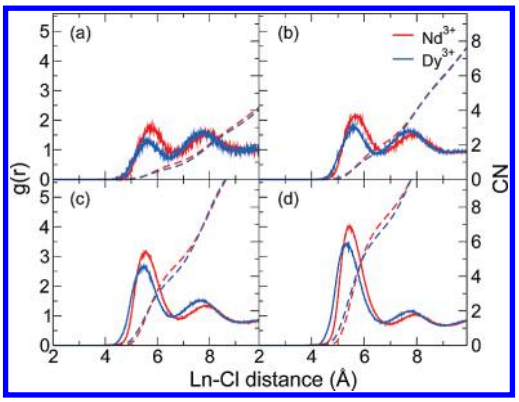


**Figure 3.** Ln−Cl radial distribution functions (solid lines) and coordination number (dashed lines) obtained for binary aqueous solutions of $Nd(ClO_4)_3$ (red) and $Dy(ClO_4)_3$ (blue) at different concentrations: (a) 0.5, (b) 1.0, (c) 2.0, and (d) 3.0 mol $kg^{-1}$.

to $Nd^{3+}$ leave its first hydration shell, respectively at 200, 500, and 1700 ps, leading to a total dissociated $Nd^{3+}/3NO_3^-$ salt after 1.7 ns. No salt dissociation has been observed for $Dy^{3+}$ on our simulation time scale, certainly due to the slower dynamics of water molecules in the neighborhood of $Dy^{3+}$.

Analyzing the simulation part where the nitrate anions are coordinated to the lanthanide cation in highly diluted solution, we noticed two peaks corresponding to the first hydration shell on the Ln−N RDFs (Figure 2). As mentioned for perchlorate anions, nitrate anions are able to adopt different coordination modes with $Ln^{3+}$: (i) monodentate (with a Ln−N distance of 3.70 Å for $Nd^{3+}$ and 3.57 Å for $Dy^{3+}$) and (ii) bidentate (with a Ln−N distance of about 3 Å for $Nd^{3+}$ and 2.88 Å for $Dy^{3+}$). From the Ln−N RDFs, it appears clearly that the monodentate coordination is preferred by the $NO_3^-$ anions. Indeed, Dobler et al. have shown, by quantum chemical investigation, that increasing the number of water molecules in the $Ln^{3+}$ first coordination shell promotes the monodentate coordination of nitrate in the $Ln^{3+}$ first coordination shell.[48] Furthermore, from MD simulations without polarization, the change from bidentate to monodentate coordination is also observed before the salt dissociation.[48]

However, the RDFs also show that the bidentate mode is slightly more stable for $Nd^{3+}$ than for $Dy^{3+}$. Simulations have also been performed for other $Ln^{3+}$ cations, that is, $La^{3+}$, $Eu^{3+}$, and $Lu^{3+}$, in order to highlight the evolution of the nitrate affinity for $Ln^{3+}$ ions in the series (Supporting Information Figure S1). These simulations show that going to the end of the lanthanide series decreases the ratio between bidentate and monodentate conformations, this ratio being equal to zero for the heaviest lanthanide, $Lu^{3+}$. Moreover, as observed for the lanthanide perchlorates, the monodentate conformation promotes the lanthanide nitrate salt dissociation. These results are consistent with the decrease of the experimental values of $Ln^{3+}-NO_3^-$ association constant in the lanthanide series:[43,44] at the end of the lanthanide series, nitrate anions promote the monodentate conformation leading to the salt dissociation.

**3.2. Structural Properties of Lanthanide Salt Concentrated Aqueous Solutions.** We present here the first and second coordination shell structures obtained for the $Nd^{3+}$ and $Dy^{3+}$ perchlorate, chloride, and nitrate salt concentrated aqueous solutions. As explained above, we simulated lanthanide salt solutions starting from a first-shell-dissociated conformation at different concentrations (Figure 1). Characteristics of the simulation boxes are given in Table 2. Note that, at the highest concentration (3.0 mol $kg^{-1}$), the total number of water molecules per $Ln^{3+}$ ion (18.5) is smaller than the hydration number of $Ln^{3+}$ in the two first hydration shells in pure water (28 and 26 for $Nd^{3+}$ and $Dy^{3+}$, respectively).

**3.2.1. Structural Properties of the First Coordination Shells. $Nd^{3+}$ Salts.** The presence of perchlorate anions in $Nd^{3+}$ aqueous solutions has no influence on the $Nd^{3+}$ first hydration shell structure (Figure 3). Indeed, no perchlorate anion has been observed in this shell, even at high concentrations (Table 3). Moreover, the $Nd-O_W$ distance and the number of water molecules in its first hydration shell do not vary as a function of the concentration, that is, 8.8−8.9 water molecules at 2.52 Å.

$Nd^{3+}$ chloride salts are also mainly totally dissociated, with no anion in the cation first coordination shell (Figure 4); the $Nd-O_W$ distance and the CN in the first hydration shell (8.8 $H_2O$ at 2.52 Å) do not vary. However, $Cl^-$ anions are found in the $Nd^{3+}$ first hydration shell at 3.0 mol $kg^{-1}$, but in small amounts: only one $Nd^{3+}-Cl^-$ inner-sphere pair, despite the 192 $Cl^-$'s present in solution, has been observed (Table 3), explaining the small peak at 2.68 Å on the Nd−Cl RDF.

Simulations of $Nd^{3+}$ nitrate solutions were performed at different concentrations using the same methodology. Contrary to the observations made for perchlorate and chloride salts, raising the $Nd^{3+}$ nitrate concentration in solution has an effect on the $Nd^{3+}$ first coordination shell properties (Figure 5). Indeed, the number of nitrates progressively increases in this shell from 0.1 at 0.5 mol $kg^{-1}$ to 0.6 at 3.0 mol $kg^{-1}$ (Table 3). However, we must notice that this association remains weak, since at the highest concentration the total number of nitrates in the $Nd^{3+}$ first coordination shell is less than 1. This is consistent with small experimental values of the association constant of $Nd^{3+}$ (0.8,[42] 0.64[45]) and others $Ln^{3+}$[81] with nitrate. This increase leads to a decrease in the number of water molecules in the first coordination

(81) Bünzli, J.-C. G.; Yersin, J.-R. *Inorg. Chem.* **1979**, *18*, 605–607.

**Table 3.** Hydration Properties of $Nd^{3+}$ in Aqueous Solution at Room Temperature

| | $r_{Nd-O_w}{}^{(1)a}$ | $CN_{wat}^{(1)\,b}$ | $r_{Nd-O_w}{}^{(2)a}$ | $CN_{wat}^{(2)\,b}$ | $r_{Nd-Cl}^{(1)\,c}$ | $CN_{PER}^{(1)\,d}$ | $r_{Nd-Cl}^{(2)\,c}$ | $CN_{PER}^{(2)\,d}$ | $MRT_{PER}^{(2)\,e}$ |
|---|---|---|---|---|---|---|---|---|---|
| | | | | $Nd(ClO_4)_3$ | | | | | |
| Sim(D) | 2.52 | 8.7 | 4.72 | 18.9 | | | 5.5 | 0.1 | 16 |
| Sim(0.5) | 2.52 | 8.8 | 4.72 | 18.0 | | | 5.78 | 1.0 | 14 |
| Sim(1) | 2.52 | 8.8 | 4.71 | 16.6 | | | 5.69 | 2.1 | 16 |
| Sim(2) | 2.52 | 8.9 | 4.69 | 13.6 | | | 5.55 | 4.8 | 23 |
| Sim(3) | 2.53 | 8.9 | 4.68 | 9.8 | | | 5.45 | 7.7 | 38 |
| | | | | $NdCl_3$ | | | | | |
| Sim(D) | 2.52 | 8.8 | 4.72 | 18.0 | | | 5 | 0.2 | 26 |
| Sim(0.5) | 2.52 | 8.7 | 4.72 | 17.7 | | | 5.06 | 1.0 | 27 |
| Sim(1) | 2.52 | 8.7 | 4.72 | 16.4 | | | 5.05 | 2.0 | 33 |
| Sim(2) | 2.52 | 8.7 | 4.73 | 13.6 | | | 5.04 | 4.0 | 42 |
| Sim(3) | 2.51 | 8.6 | 4.72 | 11.3 | 2.68 | < 0.1 | 5.05 | 5.9 | 56 |
| | | | | $Nd(NO_3)_3$ | | | | | |
| Sim(D) | 2.52 | 8.8 | 4.72 | 18.7 | | | 5.0−5.5 | 0.1 | 19 |
| Sim(0.5) | 2.52 | 8.7 | 4.72 | 17.5 | $3^{bi}/3.70^{mo}$ | $0.1^{mo}$ | 5.3−5.6 | 1.1 | 26 |
| Sim(1) | 2.52 | 8.7 | 4.72 | 15.9 | $3^{bi}/3.70^{mo}$ | $0.1^{mo}$ | 5.3−5.6 | 2.5 | 31 |
| Sim(2) | 2.53 | 8.5 | 4.71 | 13.1 | $3^{bi}/3.70^{mo}$ | $0.4^{mo}$ | 5.2−5.6 | 4.7 | 45 |
| Sim(3) | 2.53 | 8.4 | 4.71 | 10.4 | $3^{bi}/3.70^{mo}$ | $0.6^{mo}$ | 5.2−5.5 | 6.0 | 66 |

[a] First ($r_{Nd-O_w}{}^{(1)}$) and second ($r_{Nd-O_w}{}^{(2)}$) maximum peaks of Nd−$O_W$ RDFs (in Å). [b] Coordination number of the first ($CN_{wat}^{(1)}$) and the second ($CN_{wat}^{(2)}$) hydration shells. [c] First ($r_{Nd-X}^{(1)}$) and second ($r_{Nd-X}^{(2)}$) maximum peaks of Nd−X (X = Cl or N) RDFs (in Å). Superscripts bi and mo correspond to the bidentate and the monodentate nitrato conformations, respectively. [d] Number of anions in the first ($CN_A^{(1)}$) and the second ($CN_A^{(2)}$) hydration shells of $Nd^{3+}$. Superscripts bi and mo correspond to the bidentate and the monodentate nitrato conformations, respectively. [e] Mean residence times of anions ($MRT_A^{(2)}$) in the $Nd^{3+}$ second hydration shell (in ps).

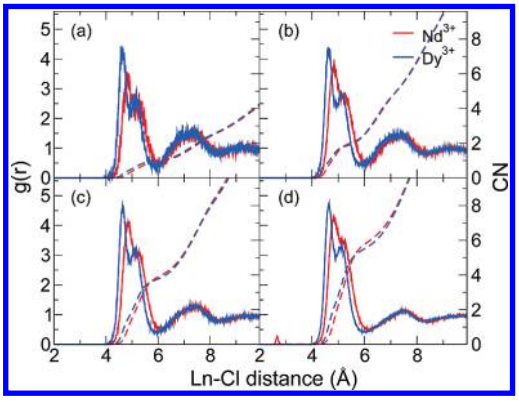


**Figure 4.** Ln−Cl radial distribution functions (solid lines) and coordination number (dashed lines) obtained for binary aqueous solutions of $NdCl_3$ (red) and $DyCl_3$ (blue) at different concentrations: (a) 0.5, (b) 1.0, (c) 2.0, and (d) 3.0 mol $kg^{-1}$.

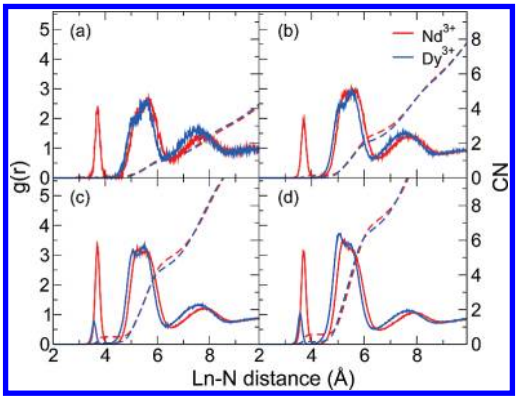


**Figure 5.** Ln−N radial distribution functions (solid lines) and coordination numbers (dashed lines) obtained for binary aqueous solutions of $Nd(NO_3)_3$ (red) and $Dy(NO_3)_3$ (blue) solutions at different concentrations: (a) 0.5, (b) 1.0, (c) 2.0, and (d) 3.0 mol $kg^{-1}$.

shell, without any modifications of the Ln−$O_W$ distance (2.52 Å). Furthermore, from a dynamic point of view, $NO_3^-$ exchange processes with water molecules have been observed at each concentration between the $Nd^{3+}$ first and second coordination shells. As mentioned for highly diluted solutions, two nitrate anion binding modes are observed on the Nd−N RDFs (about 3 Å for the bidentate one and 3.7 Å for the monodentate one). However, very few bidentate conformations are observed (the integration of the RDFs for the bidentate conformation gives an average coordination number less than 0.1).

UV−visible experiments have been performed for a binary solution of $Nd(NO_3)_3$ and $NdCl_3$. Figure 6 compares the spectra obtained for these solutions to the spectrum of $Nd^{3+}$ diluted in a $HClO_4$ solution. As previously observed for $DyCl_3$ binary salt solutions,[14] even at high concentrations, there is no indication of inner-sphere complexation between $Nd^{3+}$ and $Cl^-$. However, for the binary $Nd(NO_3)_3$ solutions, the 574 and 732 nm transitions are modified (in terms of maximum absorption wavelength, fwhm, and molar extinction coefficient), showing the presence of nitrates in the $Nd^{3+}$ first coordination sphere (Figure 7), in agreement with our MD simulations.

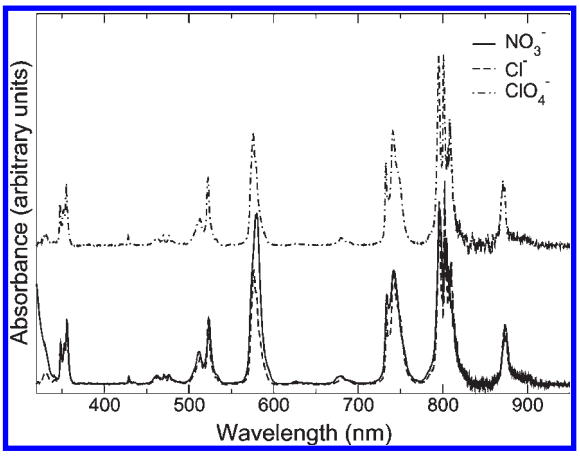


**Figure 6.** Normalized UV−visible/near-IR spectra: solutions of $Nd(NO_3)_3$ (2.7 mol $kg^{-1}$, solid line), $NdCl_3$ (3.1 mol $kg^{-1}$, dashed line), and $Nd(ClO_4)_3$ (dot dashed line). Assignments of the bands can be found in refs 84−86.

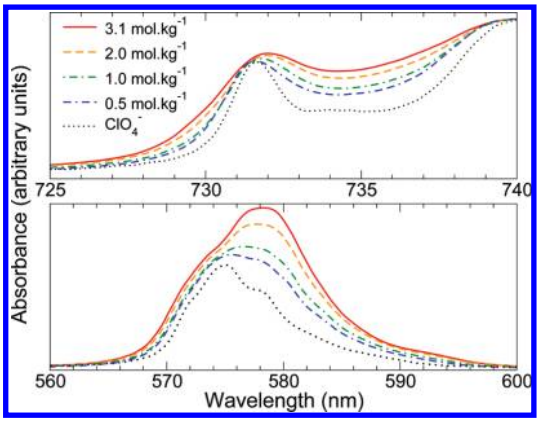


**Figure 7.** Normalized $Nd(NO_3)_3$ UV−visible/near-IR spectra variation as a function of the concentration: 3.1 (red), 2.0 (orange), 1.0 (green), and 0.5 mol $kg^{-1}$ (blue), at 732 nm (top) and 574 nm (bottom). $Nd^{3+}$ in $HClO_4$ medium UV−visible/near-IR spectrum (dots) is presented as a comparison. Assignments of the bands can be found in refs 84−86.

**$Dy^{3+}$ Salts.** As observed for the $Nd^{3+}$ perchlorate and chloride salts, these anions have no influence on the $Dy^{3+}$ first coordination shell (Table 4). The Dy−$O_W$ distance does not vary whatsoever the concentration of the binary solution (2.39 Å) or the number of water molecules (8.0) in this shell.

Contrary to $Nd^{3+}$ nitrate salt solutions, the first shell association between $Dy^{3+}$ and nitrate anions is only observed above the concentration of 2.0 mol $kg^{-1}$, with about 0.1 $NO_3^-$ per $Dy^{3+}$ at 2.0 mol $kg^{-1}$ and 0.2 at 3.0 mol $kg^{-1}$. As for $Nd^{3+}$, the presence of nitrate anions in the $Dy^{3+}$ first coordination shell leads to a small decrease in the average number of water molecules in that shell (from 8 to 7.9) with no change in the Dy−$O_W$ distance (2.39 Å). Moreover, the fact that only one peak (centered at 3.57 Å) is observed in the Dy−N RDFs (Figure 5) is consistent with the nitrate ions binding exclusively monodentate to $Dy^{3+}$, as already mentioned for highly diluted solutions. However, even for the two highest concentrations, the calculated number of nitrate anions in the $Dy^{3+}$ first coordination remains very small compared to what was observed for $Nd^{3+}$.

Concerning the UV−visible experiments, the $Dy(NO_3)_3$ spectrum analysis at a high concentration (2.7 mol $kg^{-1}$) and its comparison to the $Dy(ClO_4)_3$−$HClO_4$ solution spectrum show that the band properties are not modified. The similarity of the spectra indicates that nitrate ions do not form inner-sphere complexes with $Dy^{3+}$, even at high concentrations (Supporting Information Figure S2). The same observation was made for $DyCl_3$ in a previous work.[14]

**3.2.2. Structural Properties of the Lanthanide Second Coordination Shells. $Nd^{3+}$ Salts.** For the three anions (perchlorate, chloride, and nitrates), the structural properties are very similar. Although the Nd−$O_W$ distance does not vary much as a function of the concentration in this shell, the number of water molecules decreases, going from about 20 to 10. This decrease is due to the increasing number of anions in that shell, going from 0.1 to 8, depending on the anion (Table 3). Note that the Nd−$O_W$ distances calculated in the second coordination shell for the three anions (4.68−4.73 Å) are almost the same as the one calculated in pure liquid water (4.73 Å), pointing out the weak influence of anions on the water molecule structure in the $Nd^{3+}$ second coordination shell.

However, contrary to perchlorates, Nd−Cl RDFs reveal that at each concentration two peaks can be distinguished in the second coordination shell (Figure 4). These two peaks correspond to two different positions of chloride ions in this shell, which are hydrogen-bonded to the water molecules in the $Nd^{3+}$ first coordination shell. At 4.78−4.79 Å, the chloride anion forms two H bonds with two different water molecules of the first coordination shell, namely, "$2H_W$−1Cl" (Figure $8c_1$), whereas, at 5.25−5.29 Å, $Cl^-$ forms only one H bond with one water molecule of the first coordination shell, namely, "$1H_W$−1Cl" (Figure $8c_2$).

For $Nd(NO_3)_3$ salts, a broad peak is observed on the Nd−N RDFs, corresponding to the second coordination shell (Figure 5). This peak has been attributed to different orientations of nitrate anions in the second coordination shell. As observed for chloride, the location of nitrate in the second coordination shell depends on the number of oxygens of the nitrate anion involved in H bonds with $Ln^{3+}$ first coordination shell water molecules. One nitrato oxygen makes (i) one H bond with one water molecule belonging to the $Nd^{3+}$ first coordination shell ("$1H_W$−$1O_N$"; Figure $9c_3$), (ii) two H bonds with two different water molecules being in the $Nd^{3+}$ first coordination shell ("$2H_W$−$1O_N$"; Figure $9c_2$). We also observed two nitrato oxygens making two H bonds with two different water molecules being in the $Nd^{3+}$ first coordination shell ("$2H_W$−$2O_N$"; Figure $9c_1$). Note that the splitting (in two peaks), observed for nitrates and chlorides and not for perchlorates, points out a weaker H-bonding with perchlorate anions than with nitrate and chloride anions, confirming the spectator role of perchlorate anions.

**$Dy^{3+}$ Salts.** As already observed for $Nd^{3+}$ salts, increasing the concentration of the binary solutions leads to the increase of the number of anions in the $Dy^{3+}$ second coordination shell. Structures obtained for $Dy^{3+}$ perchlorate, chloride, and nitrate salts are almost the same. Indeed, for the three types of salts, the number of water molecules decreases as the number of anions increases in the second coordination shell, from 20 to about 10.

**Table 4.** Hydration Properties of $Dy^{3+}$ in Aqueous Solution at Room Temperature

| | $r_{Dy-O_w}^{(1)a}$ | $CN_{wat}^{(1)b}$ | $r_{Dy-O_w}^{(2)a}$ | $CN_{wat}^{(2)b}$ | $r_{Dy-Cl}^{(1)c}$ | $CN_{PER}^{(1)d}$ | $r_{Dy-Cl}^{(2)c}$ | $CN_{PER}^{(2)d}$ | $MRT_{PER}^{(2)e}$ |
|---|---|---|---|---|---|---|---|---|---|
| | | | | $Dy(ClO_4)_3$ | | | | | |
| Sim(D) | 2.39 | 8.0 | 4.59 | 18.1 | | | | | |
| Sim(0.5) | 2.39 | 8.0 | 4.58 | 17.0 | | | 5.68 | 0.6 | 12 |
| Sim(1) | 2.39 | 8.0 | 4.57 | 15.8 | | | 5.61 | 1.6 | 14 |
| Sim(2) | 2.39 | 8.0 | 4.55 | 13.0 | | | 5.46 | 4.0 | 21 |
| Sim(3) | 2.39 | 8.0 | 4.53 | 9.9 | | | 5.33 | 6.7 | 34 |
| | | | | $DyCl_3$ | | | | | |
| | $r_{Dy-O_w}^{(1)a}$ | $CN_{wat}^{(1)b}$ | $r_{Dy-O_w}^{(2)a}$ | $CN_{wat}^{(2)b}$ | $r_{Dy-Cl}^{(1)c}$ | $CN_{Cl}^{(1)d}$ | $r_{Dy-Cl}^{(2)c}$ | $CN_{Cl}^{(2)d}$ | $MRT_{Cl}^{(2)e}$ |
| Sim(D) | 2.39 | 8.0 | 4.59 | 17.8 | | | 4.6 - 4.8 | 0.1 | 29 |
| Sim(0.5) | 2.39 | 8.0 | 4.59 | 16.0 | | | 4.90 | 1.0 | 45 |
| Sim(1) | 2.39 | 8.0 | 4.59 | 15.4 | | | 4.89 | 1.9 | 42 |
| Sim(2) | 2.39 | 8.0 | 4.59 | 13.2 | | | 4.89 | 3.8 | 54 |
| Sim(3) | 2.39 | 8.0 | 4.60 | 11.2 | | | 4.90 | 5.6 | 71 |
| | | | | $Dy(NO_3)_3$ | | | | | |
| | $r_{Dy-O_w}^{(1)a}$ | $CN_{wat}^{(1)b}$ | $r_{Dy-O_w}^{(2)a}$ | $CN_{wat}^{(2)b}$ | $r_{Dy-N}^{(1)c}$ | $CN_{NIT}^{(1)d}$ | $r_{Dy-N}^{(2)c}$ | $CN_{NIT}^{(2)d}$ | $MRT_{NIT}^{(2)e}$ |
| Sim(D) | 2.39 | 8.0 | 4.58 | 19.9 | | | 5.0−5.5 | 0.2 | 60 |
| Sim(0.5) | 2.39 | 8.0 | 4.58 | 16.4 | | | 5.0−5.6 | 1.0 | 30 |
| Sim(1) | 2.39 | 8.0 | 4.57 | 15.0 | | | 5.0−5.5 | 2.2 | 33 |
| Sim(2) | 2.39 | 7.9 | 4.56 | 12.6 | $3.57^{mo}$ | $0.1^{mo}$ | 5.0−5.5 | 4.4 | 47 |
| Sim(3) | 2.39 | 7.9 | 4.55 | 9.8 | $3.57^{mo}$ | $0.2^{mo}$ | 5.0−5.5 | 6.6 | 67 |

[a] First ($r_{Dy-O_w}^{(1)}$) and second ($r_{Dy-O_w}^{(2)}$) maximum peaks of Dy−$O_W$ RDFs (in Å). [b] Coordination number of the first ($CN_{wat}^{(1)}$) and the second ($CN_{wat}^{(2)}$) hydration shells. [c] First ($r_{Dy-X}^{(1)}$) and second ($r_{Dy-X}^{(2)}$) maximum peaks of Dy−X (X = Cl or N) RDFs (in Å). Superscripts bi and mo correspond to the bidentate and the monodentate nitrato conformations, respectively. [d] Number of anions in the first ($CN_A^{(1)}$) and the second ($CN_A^{(2)}$) hydration shells of $Dy^{3+}$ . Superscripts bi and mo correspond to the bidentate and the monodentate nitrato conformations, respectively. [e] Mean residence times of anions ($MRT_A^{(2)}$) in the $Dy^{3+}$ second hydration shell (in ps).

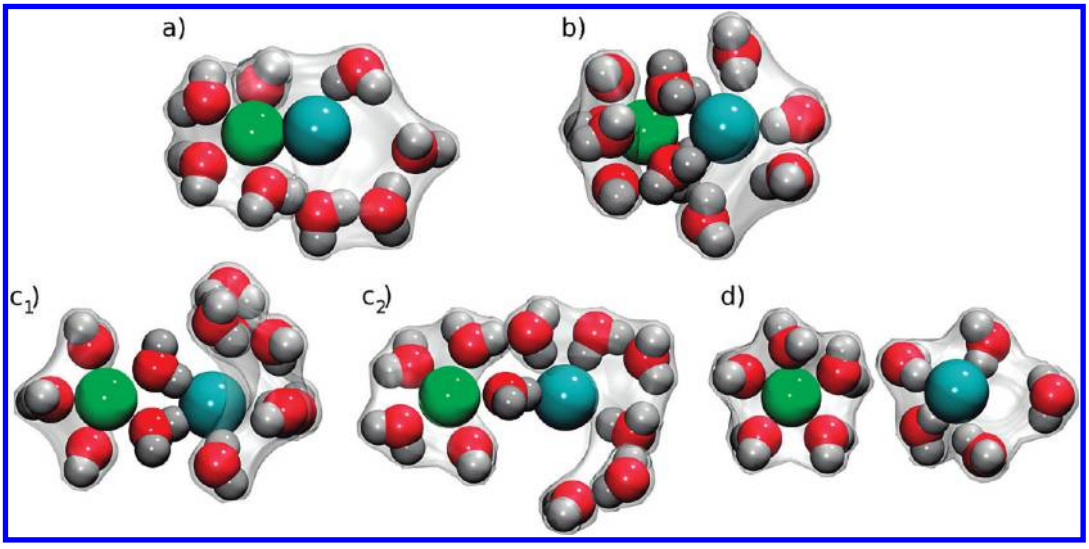


**Figure 8.** Characteristic locations of $Cl^-$ (blue) around $Nd^{3+}$ (green) observed from the potential of mean force profile of $Nd^{3+}$−$Cl^-$ in water (Figure 10): (a) in the first coordination shell (2.68 Å), (b) at the first maximum (3.35 Å), ($c_1$ and $c_2$) in the second coordination shell (4.74 and 5.32 Å), and (d) in the third coordination shell (7.67 Å).
For clarity reasons, the snapshots are represented like 2D snapshots. Therefore, only significant water molecules are represented.

For the chloride salts, the two positions of chloride in the second coordination shell are also observed: the "$2H_W$−1Cl" conformation is located at 4.64−4.65 Å and the "$1H_W$−1Cl" one at 5.10−5.12 Å.

For $Dy(NO_3)_3$, as for $Nd^{3+}$, the Dy−N RDFs show also a broad peak describing the second coordination shell (Figure 5) and corresponding to the three previously mentioned conformations of nitrates in the $Ln^{3+}$ second coordination shell.

## 4. Discussions

The influence of the concentration of binary lanthanide salt solutions on the structural properties of $Nd^{3+}$ and $Dy^{3+}$ in aqueous solutions has been studied. We highlight

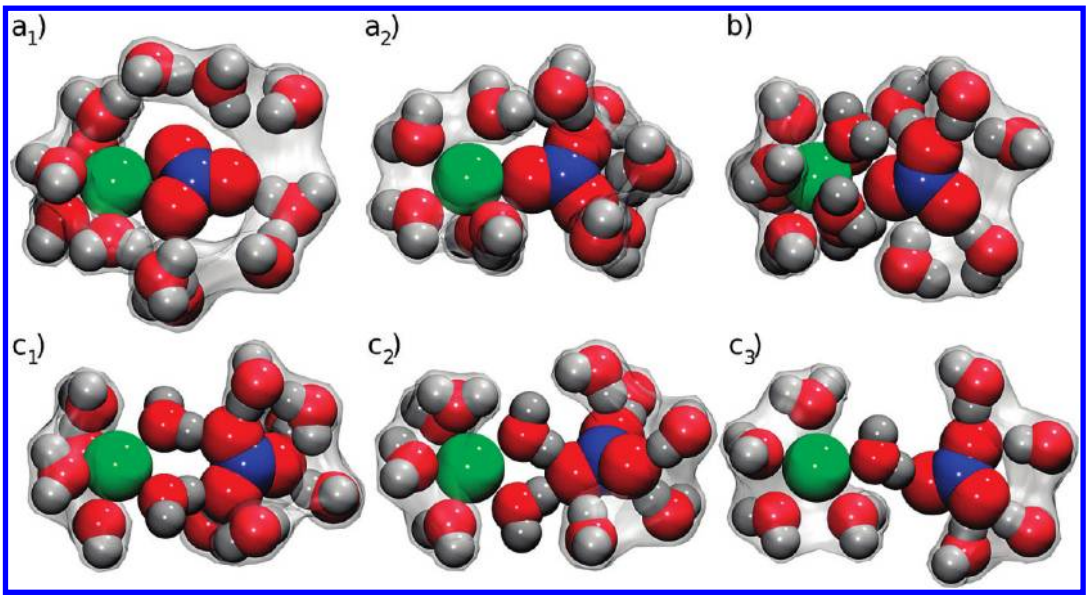


**Figure 9.** Characteristic locations of $NO_3^-$ around $Nd^{3+}$ (green) observed from the potential of mean force profile of $Nd^{3+}-NO_3^-$ in water (Figure 11): ($a_1$ and $a_2$) in the first coordination shell (3.01 and 3.70 Å), (b) at the first maximum (4.20 Å), ($c_1$, $c_2$, and $c_3$) in the second coordination shell (5.05, 5.40, and 5.75 Å, respectively).
For clarity reasons, the snapshots are represented like 2D snapshots. Therefore, only significant water molecules are represented.

differences and similarities in their first and second coordination shell structural properties.

Independently of the concentration, in the present MD simulations, no first shell association is observed between the $Ln^{3+}$ ions and the chloride/perchlorate anions, which is in agreement with UV visible experiments. However, nitrate anions are observed in the $Dy^{3+}$ first coordination shell above 2.0 mol $kg^{-1}$, and for all simulated solutions (from 0.5 mol $kg^{-1}$ to 3.0 mol $kg^{-1}$) in the case of $Nd^{3+}$. The presence and increase of the first shell association between $Nd^{3+}$ and nitrate, observed from MD simulations, are in good agreement with the UV visible results. For $Dy^{3+}$, the very weak first shell association with nitrate anions observed from the MD simulations is in a reasonable agreement with the UV visible experiments, indicating a negligible or very weak inner-sphere association with nitrate anions. The weaker first shell association between $Dy^{3+}$ and nitrate can be explained by the total number of water molecules present in solution. Indeed, $Dy^{3+}$ needs less water molecules than $Nd^{3+}$ to complete its first hydration shells (the first and the second one). As the number of water molecules per lanthanide, at the highest concentration (3 mol $kg^{-1}$), is small (18.5), we may suppose that the competition between the nitrate hydration and the $Ln^{3+}$ hydration is weaker in the case of $Dy^{3+}$ than in that of $Nd^{3+}$. Thus, the number of water molecules in solution is almost sufficient to hydrate $Dy^{3+}$ ions and nitrates, whereas that is not the case for $Nd^{3+}$, and consequently some nitrate anions enter the $Nd^{3+}$ first coordination shell. The $Nd^{3+}$ and $Dy^{3+}$ first coordination shell structural properties allow then a highlighting of (i) the stronger affinity of nitrate anions toward $Ln^{3+}$ ions compared to perchlorate and chloride anions and (ii) a stronger affinity of nitrates for $Nd^{3+}$ than for $Dy^{3+}$, in agreement with experimental values of nitrate association constants determined by microcalorimetry,[43] extraction,[44] and the present UV visible study.

Looking at the $Ln^{3+}$ second coordination shell structures, almost the same anion behaviors are observed, that is, an increase in the number of anions in the second coordination shell as a function of the concentration leading to a decrease in the number of water molecules in this shell without any change in the $Ln-O_W^{(2)}$ distance.

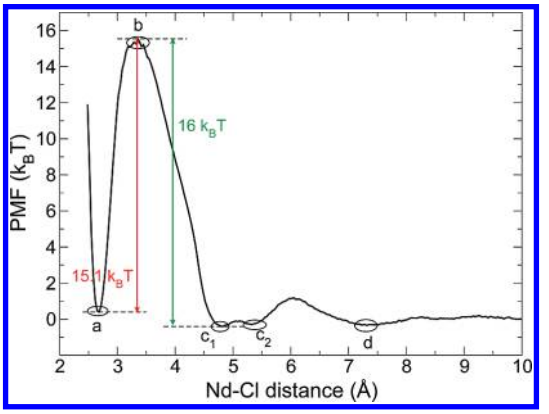


**Figure 10.** Potential of mean force profile of $Nd^{3+}-Cl^-$ in water and characteristic locations of $Cl^-$ (Figure 8).

In order to cast light on the dissociation/association processes of these salts, some umbrella-sampling molecular dynamics simulations have been performed for $Nd^{3+}-Cl^-$ and $Nd^{3+}-NO_3^-$ ion pairs in aqueous solution. These simulations allow the construction of free energy PMF profiles and a correlation of these profiles with corresponding geometries. These PMFs could be used to evaluate ion pair association constants, but it would be difficult to relate them with pairing at a high concentration, since they are calculated at high dilution. The PMF issuings, reported in Figures 10 and 11, for $Nd^{3+}-Cl^-$ and $Nd^{3+}-NO_3^-$, respectively, clearly show the different behaviors of these two anions toward $Nd^{3+}$ in aqueous solution.

For a chloride anion to move from the first to second coordination shell of $Nd^{3+}$, it requires crossing a 15.1 $k_BT$ barrier (Figure 10), whereas for a nitrate ion, this barrier is only 4.8 $k_BT$ (Figure 11). This difference may explain why the total dissociation was not observed in our simulation time

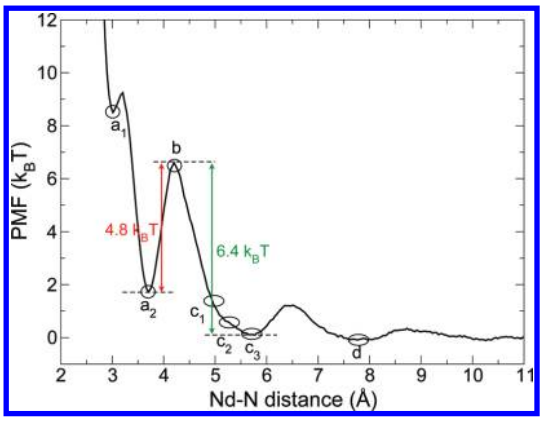


**Figure 11.** Potential of mean force profile of $Nd^{3+}-NO_3^-$ in water and characteristic locations of $NO_3^-$ (Figure 9). Note that the (d) location looks like the (d) one obtained for $Cl^-$ (Figure 8).

range (2 ns) for $NdCl_3$ first-shell-associated salts. The reverse transition (from the second to its first coordination shell) presents also an important difference between both anions: 16 $k_BT$ is needed for a chloride ion to enter the $Nd^{3+}$ first coordination shell, while only 6.4 $k_BT$ is sufficient for a nitrate anion.

The $Nd^{3+}-Cl^-$ PMF profile shows that, for a chloride ion to enter the first coordination shell of $Nd^{3+}$, it must first move from a $1H_W-1Cl$ conformation to that of a $2H_W-1Cl$ (Figure $8c_1$ and $c_2$). The latter conformation precludes the entrance into the $Nd^{3+}$ first shell by stabilizing and moving closer the two water molecules located between the anion and the cation in the $2H_W-1Cl$ conformation ($d_{O_W-O_W} = 2.8$ and 3 Å for the $2H_W$ and $1H_W$, respectively). For this transition of $Cl^-$ from the second to the first cation shell, the energy barrier to cross is therefore more important than for $NO_3^-$. A conformational analysis for the identical nitrate ion transition shows that $NO_3^-$ uses a series of energetically closed intermediate conformations to enter into the $Nd^{3+}$ first shell. The geometry of that anion allows it to rotate around its central nitrogen in order to adopt successively the $1H_W-1O_N$ or $2H_W-2O_N$ conformation in the second shell, permitting a concomitant approach in the cation first shell (Figure $9c_1$ and $c_2$). Furthermore, contrary to what is observed for $Cl^-$, this approach also involves an opening of the water molecules "sandwiched" between the two ions ($d_{O_W-O_W} = 2.9$ and 3.1 Å for the $2H_W-1O_N$ and $2H_W-2O_N$, respectively). These exchange processes using multiple intermediate conformations explain why, in the case of $NO_3^-$, the energy barriers are smaller than for $Cl^-$ .

As mentioned above, the nitrate ion can adopt two different coordination modes as it binds to a $Ln^{3+}$ ion: bidentate or monodentate. Although, in solid nitrato compounds of $Ln^{3+}$, the nitrate anion is mainly bidentate,[82,83] its coordination mode has been the subject of controversial interpretations in aqueous solutions.[40,45,48] Indeed, Yaita et al. suggest, from EXAFS spectroscopy, a bidentate nitrato coordination for almost the entire series of $Ln^{3+}$ ions (from $Nd^{3+}$ to $Lu^{3+}$), but these results were obtained for a very high concentration of $HNO_3$ (13 mol $L^{-1}$).[40] Recently, Rao and Tian have also proposed a bidentate nitrato coordination through the $Ln^{3+}$ series from luminescence spectroscopy.[45] On the other hand, Dobler et al. showed, from quantum calculations and MD simulations without explicit polarization, that the monodentate and bidentate coordinations become energetically similar, when the first coordination shell is saturated with water molecules.[48] They also pointed out a preference for the monodentate coordination mode when going to the end of the lanthanide series. Simulation of the monocomplex $Nd(NO_3)^{2+}$ has been performed in water in order to probe the nitrate anion coordination (mono- or bidentate) mode with $Nd^{3+}$ when there is only one nitrate ion in $Nd^{3+}$ first coordination shell. In this 2 ns simulation, the nitrate anion coordinates $Nd^{3+}$ only in a monodentate fashion (over about 400 ps) and then dissociates. The average number of water molecules in the $Nd^{3+}$ first coordination is 7.8 when (monodentate) $NO_3^-$ is located in the first shell and 8.8 when it is not. This means that a monodentate nitrate substitutes one water molecule. The $Nd^{3+}-NO_3^-$ PMF profile calculated here allows discriminating, within our model, in favor of the monodentate coordination mode ($a_2$ in Figure 9), which is 7.6 $k_BT$ lower in energy than the bidentate one ($a_1$ in Figure 9), with a very small energy barrier between the two.

From $Nd^{3+}-Cl^-$ and $Nd^{3+}-NO_3^-$ PMFs, we observe that chloride and nitrate inner-sphere binding is energetically similar. The energy differences between the first and the second coordination shell states are in fact equivalent for both anions (0.9 $k_BT$ for $Cl^-$ vs 1.6 $k_BT$ for $NO_3^-$). From a kinetic point of view, these PMFs clearly point out slower dissociation/association processes for chloride than nitrate, since the barrier energy is 1.5−2 times higher for $Cl^-$ than $NO_3^-$. On the other hand, for these three salts, evolutions of the structural characteristics with the increase of the concentration clearly show a stronger affinity of nitrates toward the two other anions for both $Ln^{3+}$ cations. The affinity difference between chloride and perchlorate ions is more difficult to highlight; even in the case of $Cl^-$ anions, some are found in the $Nd^{3+}$ first coordination shell at the highest concentration (3.0 mol $kg^{-1}$, see Table 3). Nevertheless, we must remember that the strongest affinity involved in aqueous solution is the one with water molecules. Indeed, in all of the studied solutions, very little first shell association is observed, and although we observed a competition between the three studied anions, the strongest is the one with the water molecules.

Furthermore, for each of the three salts, our calculations point out a stronger affinity of the anions for $Nd^{3+}$ above $Dy^{3+}$. Indeed, (i) there are always more nitrate anions in the $Nd^{3+}$ first coordination sphere, (ii) chloride anions are present in the $Nd^{3+}$ first coordination shell at the highest concentration, whereas none are in $Dy^{3+}$ one, and (iii) some $ClO_4^-$'s locate in the $Nd^{3+}$ second coordination shell from the highly diluted solution, whereas they are observed only above 0.5 L for $Dy^{3+}$.

## 5. Conclusions and Outlook

In this paper, we have presented a molecular dynamics study of concentrated binary aqueous solutions of lanthanide

(82) Rogers, R. D.; Rollins, A. N. *Inorg. Chim. Acta* **1995**, *230*, 177–183.
(83) Lees, A. M.; Kresinski, R. A.; Platt, A. W. *Inorg. Chim. Acta* **2006**, *359*, 1329–1334.
(84) Carnall, W. T.; Goodman, G. L.; Rajnak, K.; Rana, R. S. *J. Chem. Phys.* **1989**, *90*, 3443–3457.
(85) Binnemans, K.; Gorlett-Warland, D. *Chem. Phys. Lett.* **1995**, *235*, 163–174.
(86) Peijzel, P.; Meijerink, A.; Wegh, R.; Reid, M.; Burdick, G. *J. Solid State Chem.* **2005**, *178*, 448–453.

salts ($Nd^{3+}$ and $Dy^{3+}$ perchlorate, chloride, and nitrate). From MD simulations, we highlight the strong affinity of nitrate anions for $Ln^{3+}$ ions, compared to perchlorate and chloride anions, since only nitrate anions are observed in the $Ln^{3+}$ first hydration shell. This was confirmed by UV−visible experiments. Indeed, UV−visible experiments highlight an increase of the inner-sphere association between $Nd^{3+}$ and nitrate anions as a function of the concentration of the binary solution, whereas for perchlorate and chloride lanthanide salts, and dysprosium nitrate salts, no first shell association is observed. $Nd^{3+}-Cl^-$ and $Nd^{3+}-NO_3^-$ ion pair PMF calculations in aqueous solutions did not provide a clear answer on the chloride and nitrate affinity difference toward $Nd^{3+}$. Indeed, although from a kinetic point of view the inner-sphere association of $Cl^-$ (16 $k_BT$) is less favorable than the monodentate $NO_3^-$ one (6.4 $k_BT$), from a thermodynamic point of view, both are similar, within the PMF calculation uncertainty. However, since very little first shell association is observed between $Nd^{3+}$ and $Cl^-$ from MD simulations at 3.0 mol $kg^{-1}$, we may suppose that $Cl^-$ has a slightly stronger affinity than $ClO_4^-$. Thanks to the nitrate first shell association, we also show that the affinity of the studied anions for the $Nd^{3+}$ is stronger than for $Dy^{3+}$, in good agreement with experimental values of complexation constants.[43,44]

As we now have a better representation of concentrated binary aqueous solutions of lanthanide salts, the next step is a better description of such solutions in contact with organic solutions, like octanol solutions, in an attempt to better understand the solvation phenomena involved in the liquid−liquid extraction. Another direction is also the coupling between MD simulations and a thermodynamic model, like BIMSA, to improve the correlation between thermodynamics parameters (association constants, activity coefficients, etc.) and microscopic features (structures and dynamics), as previously done on $DyCl_3$.[14]

**Acknowledgment.** This work was supported by the "Agence Nationale pour la Recherche" AMPLI (Approche Multi-échelle du Partage de solutés entre phases LIquides). We are grateful to Mireille Guigue for her help in UV−visible experiments.

**Supporting Information Available:** Tables S1 and S2 and Figures S1 and S2. This material is available free of charge via the Internet at http://pubs.acs.org.